



## On-chip polariton generation using an embedded nanograting microring circuit



N. Pornsuwancharoen<sup>a</sup>, P. Youplao<sup>a</sup>, I.S. Amiri<sup>b</sup>, J. Ali<sup>c</sup>, R.R. Poznanski<sup>d</sup>, K. Chaiwong<sup>e</sup>,  
P. Yupapin<sup>f,g,\*</sup>

<sup>a</sup> Department of Electrical Engineering, Faculty of Industry and Technology, Rajamangala University of Technology Isan, Sakon Nakhon Campus, 199 Phungkon, Sakon Nakhon 47160, Thailand

<sup>b</sup> Division of Materials Science and Engineering, Boston University, Boston, MA 02215, USA

<sup>c</sup> Laser Centre, IBNU SINA ISIR, Universiti Teknologi Malaysia 81310 Johor Bahru, Malaysia

<sup>d</sup> I-CODE, Universiti Sultan Zainal Abidin, 21300 Kuala Nerus, Terengganu, Malaysia

<sup>e</sup> Department of Electrical and Electronics Engineering, Faculty of Industrial Technology, Loei Rajabhat University, Loei 42000, Thailand

<sup>f</sup> Computational Optics Research Group, Advanced Institute of Materials Science, Ton Duc Thang University, District 7, Ho Chi Minh City, Viet Nam

<sup>g</sup> Faculty of Electrical & Electronics Engineering, Ton Duc Thang University, District 7, Ho Chi Minh City, Viet Nam

### ABSTRACT

We have proposed a model of polariton generation, which is normally generated by the dipole and the strong coupling field interaction. This system consists of a gold grating embedded on the plasmonic island, which is embedded at the center of the nonlinear microring resonator, which is known as a panda-ring resonator. The strong coupling between the plasmonic waves and the grating can be formed by the whispering gallery mode (WGM) of light within a Panda-ring resonator, in which the output is a dipole-like particle known as a polariton and seen at the system output. By varying the energy of high-intensity laser pulse in the system and gold grating a strong field is generated at the output. A dipole is formed by a pair of the grating signals, where one propagates in the opposite direction of the other. By using suitable parameters, dipole-like signals can be generated. Theoretical formulation is performed for a two-level system and polariton oscillation frequency i.e., the Rabi frequency is plotted. The obtained ground and excited state frequencies of this two-level system are 187.86 and 198.20 THz, respectively.

Polariton is a particle that can be localized at the ground or excited states within the two-level system, as reported in various studies [1,2]. Photons generated by plasmonic grating can behave as charged particles in the magnetic field [3]. By using the localized surface plasmon and Bragg mode on the aluminum nanograting deposited on the aluminum film, the strong coupling could be established. In this coupling, the dipole-dipole bonds of polaritons, which are eigenstates, are generated in the interaction between the plasmonic waves and charge dipoles. In this work, we propose that the energy transfer between the polaritons generated by the interaction between plasmonic waves and whispering gallery mode (WGM) of light in the grating cavity within microring system [4,5], which can introduce the polaritons that propagate within the microring system. It is a two-level system that oscillates with Rabi frequency ( $\omega_{Rabi}$ ) [6–8], where the polariton is a particle that can be localized at the ground or excited states within the two-level system, where there are various works have been manipulated [9,10]. In Fig. 1, it is shown that the electric field  $E_{in}$  is fed into the input port along the z-axis and propagates within the system. It is defined as  $E_{in} = E_z = E_0 e^{-ik_z z - \omega t + \varphi}$ , where  $E_0$  is the initial electric field

amplitude,  $k_z$  is the wave number in the direction of propagation,  $\omega$  is the angular frequency [11–14], where  $\varphi$  is the initial phase. WGM of the coherent light is required to generate plasmonic waves within the plasmonic island within Panda-ring resonator. The electrical output field of the WGM ( $E_{WGM}$ ) can be formed by the cylindrical coordinates as described in Ref. [15]. The reflected output of the grating within the plasmonic island can be given by  $I_{WGM} = -R_{WGM} I_{WGM}$ , where  $R_{WGM}$  is the reflectivity of the applied material, for example, gold. The proposed system was simulated based on practically achievable device parameters [16,17] which are given in the captions of relevant figures. In Fig. 1, the selected wavelength from the light source is fed into the system via the input port, which is represented as input electric field ( $E_{in}$ ). The reflected grating output signal of the system is shown in Fig. 1, where the reflected light power is entered into the Panda-ring system, where the peak reflection ( $P_B(\lambda_B)$ ) at the waveguide port is approximately given by  $P_B(\lambda_B) \approx \tanh^2 \left[ \frac{N\pi(V)\delta n_0}{n} \right]$ . Here  $N$  is the number of the periodic variations,  $\delta n_0$  is the refractive index variation of the waveguide,  $n$  is the fraction of power in the waveguide core, and  $\left[ \frac{2\delta n_0 \pi}{\pi} \right] \lambda_B$ . The reflected power can also be calculated by using add port

\* Corresponding author at: Computational Optics Research Group, Advanced Institute of Materials Science, Ton Duc Thang University, District 7, Ho Chi Minh City, Viet Nam.

E-mail address: [preecha.yupapin@tdtu.edu.vn](mailto:preecha.yupapin@tdtu.edu.vn) (P. Yupapin).

<https://doi.org/10.1016/j.rinp.2018.08.004>

Received 10 July 2018; Accepted 3 August 2018

Available online 09 August 2018

2211-3797/© 2018 The Authors. Published by Elsevier B.V. This is an open access article under the CC BY license

(<http://creativecommons.org/licenses/by/4.0/>).

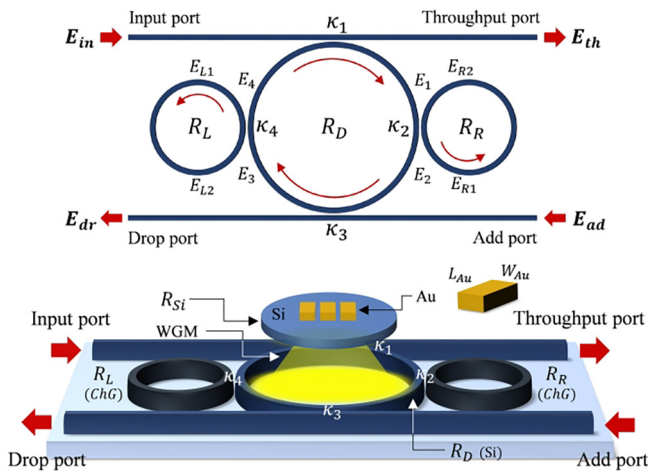


**Fig. 1.** A system of the polariton generation using the gold grating embedded in a Panda-ring resonator, where  $E_{in}$ ,  $E_{th}$ ,  $E_{dr}$ ,  $E_{ad}$  are the electrical fields of the input, throughput (through), drop and add ports.  $R_R$ ,  $R_L$ , and  $R_D$  are the right, the left, and the centre ring, respectively, the coupling coefficients  $\kappa_s = 0.5$ .  $R_{Si}$  is the silicon ring radius.  $L_{Au}$  and  $W_{Au}$  are the gold grating dimensions. The side rings are chalcogenide glass (ChG).

outputs with the criteria that the normalized power has to be maintained, where  $I_{in} = I_{th} + I_{drop} + I_{add}$  must be satisfied.

Preliminary simulation results were performed by the graphical approach of Optiwave program to obtain optimized parameters, which were subsequently used for simulations with MATLAB program. The results are presented in the aspect of the normalized condition that can be used for quantum picture presentation. The electrical field ( $E$ ) propagates within the microring system as shown in Fig. 1 is found in references [16–19]. The used waveguide loss is  $0.10 \text{ dB cm}^{-1}$ , the core effective area is  $0.30 \mu\text{m}^2$  [20,21]. The polariton excitation frequency of the two-level system can be tuned by suitable excited energy, from which the various states are formed. The probability of finding is given by the Bloch equation and expressed by  $|C_b(t)|^2 \propto \sin^2(\omega_{Rabi}t/2)$  [1,2], where  $\omega_{Rabi}$  is the Rabi frequency and  $t$  is the evolution time. From Fig. 1, the WGM light beam is generated by the Panda-ring resonator. Light propagates to the plasmonic island that has gold grating at the center. The system outputs are seen at through, drop and add ports, while the reflected light from the plasmonic grating is obtained by the add port output. The polariton oscillation distribution in the system in Fig. 1 using the Optiwave program is plotted in Fig. 2, where the input light pulse power is 50 mW with the center wavelength of  $1.55 \mu\text{m}$ . The radii of the ring system are  $R_L = R_R = 1.1 \mu\text{m}$ ,  $R_D = 2.0 \mu\text{m}$ . All  $\kappa_1$  to  $\kappa_4 = 0.5$ , the grating pitch is  $0.1 \mu\text{m}$ . The refractive index;  $n_{0ChG} = 2.9$ , the nonlinear refractive index,  $n_{2ChG} = 1.02 \times 10^{-17} \text{ m}^2 \text{W}^{-1}$  [22],  $n_{Si} = 3.47$  (Si-Crystalline silicon). The grating dimensions are (wide  $\times$  length  $\times$  thickness) =  $0.5 \mu\text{m} \times 0.5 \mu\text{m} \times 0.1 \mu\text{m}$ .  $R_{Si} = 1.6 \mu\text{m}$ , the silicon ring thickness is  $0.2 \mu\text{m}$ , where (b) is the add port output with wavelength, (c) is the add port output with time. The obtained two frequencies (excited and ground states) are 198.20 THz and 187.86 THz. The plot of the system outputs is shown in Fig. 3, where (a) throughput, (b) WGM, (c) add port, the grating pitch is ranged from 0.1 to  $0.5 \mu\text{m}$ . The input light power is fixed at 50 mW. The plot of the normalised intensity and frequency of the add port output is shown in Fig. 4, where the grating dimension is (wide  $\times$  length  $\times$  thickness) =  $0.5 \mu\text{m} \times 0.5 \mu\text{m} \times 0.1 \mu\text{m}$ , with the various input power. The plot of the relationship between the probability (normalized intensity) of finding the polariton distribution within the system and  $\sin^2(\omega_{Rabi}t/2)$  is shown in Fig. 5, where the ground and excited state frequencies are 187.86 and 198.20 THz, respectively. The evolution time is from 0.0 to 1000 fs. The polaritons can be generated by the coupling between the strong electric field and the dipole-like charge within the nonlinear microring resonator known as a Panda-ring resonator. The driven

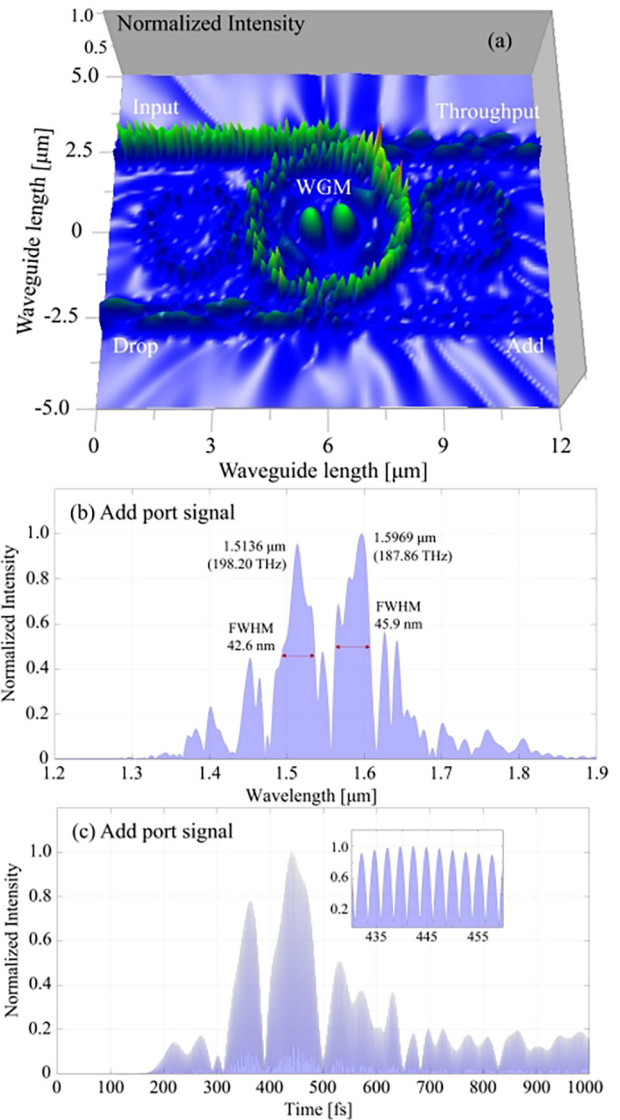


**Fig. 2.** Polariton oscillation distribution in the system in Fig. 1 using the Optiwave program, where the input light pulse power is 50 mW with the center wavelengths of  $1.55 \mu\text{m}$ .

plasmonic wave interacts with the gold grating in the island, in which charge polariton is formed by the charge dipole. The polariton can propagate within the system and be detected at the system output ports. More results are obtained at the drop and through ports, which are related to the add port outputs.

In an application, the polariton is formed by the coherent light that can transport in the same way with light within a waveguide. By using the suitable coherent light wavelength and waveguide, the polariton can transport with the long distance. The waveguide can be an optical fiber or liquid core waveguide. The latter one is very interesting, in which the polariton can transport within the liquid core waveguide that can be used for bio-cell communication [14,23], where the polariton can be transported and interacted with the ionic dipole within the microtubules, where the quasi-particle of the combined ionic dipole and polariton is formed and the information established. Principally, the polariton is generated by the human brain and transmitted to connect with the cells throughout the body, in which the information and nutrient are connected and distributed in form of the network. The plasmonic device on-chip may be possible for such a concept of operation, which may make the robot-like human called humanoid be available in the near future. The humanoid processing chip can be configured as the

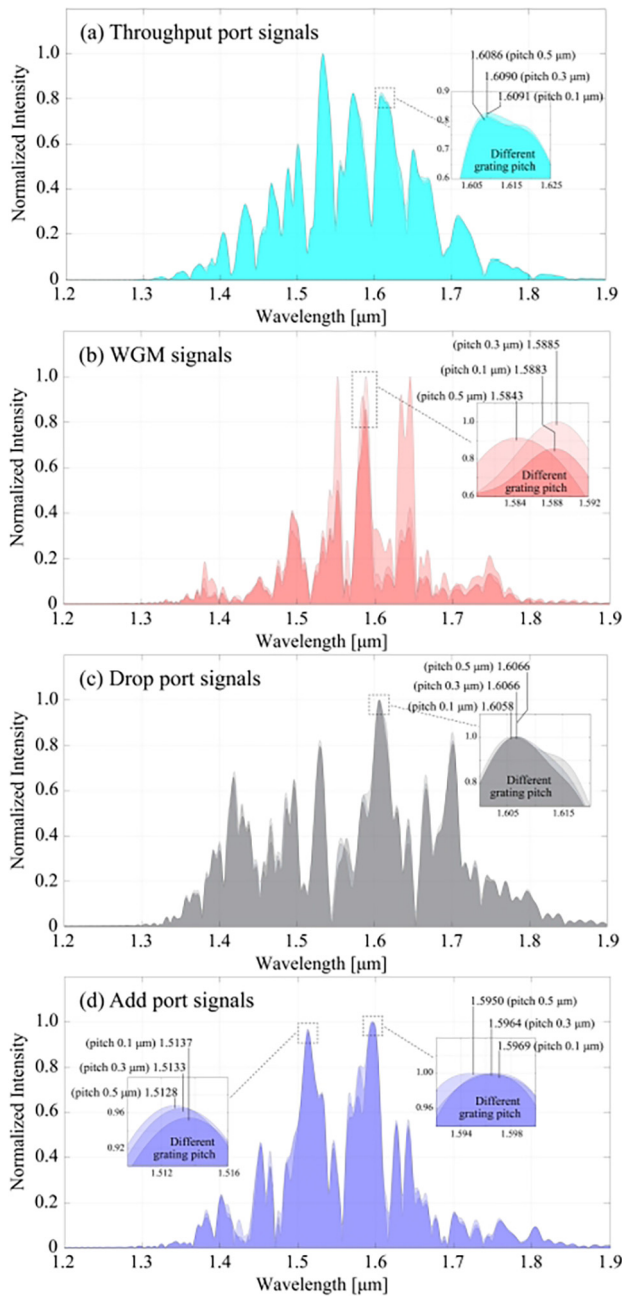


Fig. 3. The plots of the system outputs, where (a) throughput, (b) WGM, (c) add port, the grating pitch is ranged from 0.1 to 0.5  $\mu\text{m}$ , where the input light power is fixed to 50 mW.

following details. The humanoid is constructed by living cells, which is initiated by the ionic dipole. Nutrients can be injected into the system via the circuit port, which can transport into cells by the polaritons within the liquid core waveguide (blood and water). The nutrients (waste) are transported by the blood flow, while the information is transmitted via the plasmonic waves. The information can be modulated and connected to the cell networks by the polariton carrier, which can be input into the system via circuit ports. The signal code and decode (CODEC) forms can be processed by the quasi-polariton spin up and down, which is patterned to be the memory by the different magnetic field strengths. It is called the self-organised form and kept in the sub-cell region known as the subconsciousness.

Furthermore, the electro-optic conversion can be obtained by the relationship between the light intensity ( $I$ ), group velocity and the

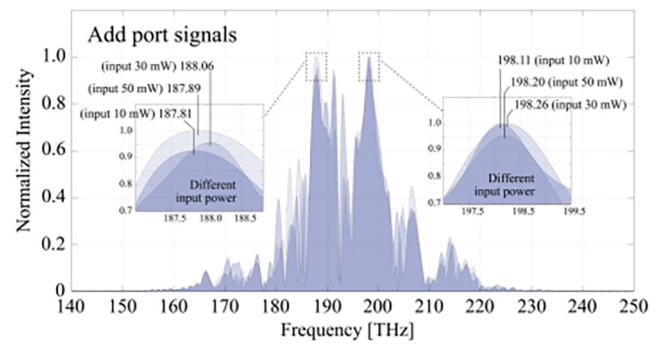


Fig. 4. The plot of the normalised intensity and frequency of the add port output, The grating dimension is (wide  $\times$  length  $\times$  thickness) = 0.5  $\mu\text{m} \times$  0.5  $\mu\text{m} \times$  0.1  $\mu\text{m}$ , with the various input power.

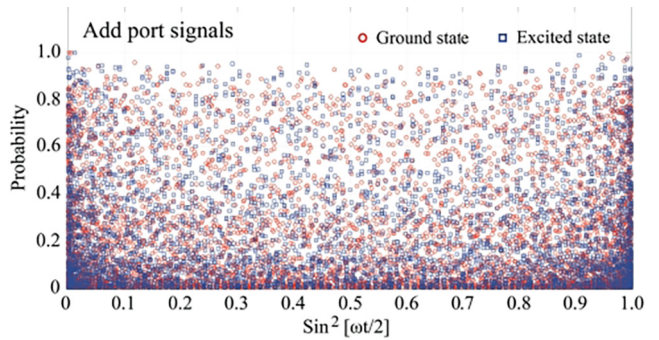


Fig. 5. The plot of the relationship between the probability (normalized intensity) of finding the polariton distribution and  $\sin^2(\omega_{Rabi}t/2)$  within the system, where the ground and excited state frequencies are 187.86 and 198.20 THz, respectively. The evolution time is from 0.0 to 1000 fs.

electron mobility, which can be expressed by  $I = E^2 = \left(\frac{V_d}{\mu}\right)^2$ , where  $V_d = \mu E$ . When an electric field  $E$  is applied to the grating sensor, an electric current is established in the gold grating. The density  $J_s$  of this current is given by  $J_s = \sigma E$ . The constant of proportionality  $\sigma$  is called the specific conductance or electrical conductivity of the conductor (gold is  $1.6 \times 10^8 \text{ W}^{-1}\text{m}^{-1}$ ) [19,24].

We have shown that the polariton can be generated by the WGM signals in the plasmonic grating, which is claimed as the interaction between charged particles and a strong electric field. The suitable grating pitch and incident WGM power can be used to form the Rabi oscillation which makes it a two-level energy transferring system. The output of such interaction is a polariton of frequency ( $\omega_{Rabi}$ ) which is a particle that moves within the Panda-ring system. The detection of such a particle can be seen at through and drop ports of the system. The probability of finding it within the system is plotted in Fig. 5 that shows convincing results. The two Rabi frequencies of the two-level system are 187.86 THz and 198.20 THz. The change in the strong field by varying the input power has shown that the Rabi frequency can be tuned and shifted, which are potentially useful for sensor applications.

#### Acknowledgments

The authors would like to give the appreciation for the research financial support and the research facilities and financial support from the Universiti Teknologi Malaysia, Johor Bahru, Malaysia through Flagship UTM shine project (03G82), Tier 1 (16H44) and Tier 2 (15J57) grants.

#### Appendix A. Supplementary data

Supplementary data associated with this article can be found, in the

online version, at <https://doi.org/10.1016/j.rinp.2018.08.004>.

## References

- [1] Gupta P, Ramakrishna SA, Wanare H. Strong coupling of surface plasmon resonances to molecules on a gold grating. *J Opt* 2016;18:105001.
- [2] Alast FH, Li G, Cheah K. Rabi-like splitting from large area plasmonic microcavity. *AIP Adv* 2017;7:085201.
- [3] Dudin Y, Li L, Bariani F, Kuzmich A. Observation of coherent many-body Rabi oscillations. *Nat Phys* 2012;8:790.
- [4] Wolverson M. Whispering resonances to the terahertz regime. AIP Publishing; 2018.
- [5] Vogt DW, Leonhardt R. Ultra-high Q terahertz whispering-gallery modes in a silicon resonator. *APL Photon* 2018;3:051702.
- [6] Ashhab S, Johansson J, Nori F. Rabi oscillations in a qubit coupled to a quantum two-level system. *New J Phys* 2006;8:103.
- [7] Sherkunov Y, Whittaker DM, Fal'ko V. Rabi oscillations of two-photon states in nonlinear optical resonators. *Phys Rev A* 2016;93:023843.
- [8] Noorden AFA, Chaudhary K, Bahadoran M, Aziz MS, Jalil MA, Tiong OC, Ali J, Yupapin P. Rabi oscillation generation in the microring resonator system with double-series ring resonators. *Optoelectron Lett* 2015;11:342–7.
- [9] Mann C-R, Sturges TJ, Weick G, Barnes WL, Mariani E. Manipulating type-I and type-II Dirac polaritons in cavity-embedded honeycomb metasurfaces. *Nat Commun* 2018;9:2194.
- [10] Lim H-T, Togan E, Kroner M, Miguel-Sanchez J, Imamoğlu A. Electrically tunable artificial gauge potential for polaritons. *Nat Commun* 2017;8:14540.
- [11] Amiri I, Naraei P, Ali J. Review and theory of optical soliton generation used to improve the security and high capacity of MRR and NRR passive systems. *J Comput Theor Nanosci* 2014;11:1875–86.
- [12] Amiri I, Alavi S, Faisal N, Supa'at A, Ahmad H. All-optical generation of two IEEE802.11n Signals for 2\$ times \$2 MIMO-RoF via MRR System. *IEEE Photon J* 2014;6:1–11.
- [13] Amiri I, Nikoukar A, Ali J. GHz frequency band soliton generation using integrated ring resonator for WiMAX optical communication. *Opt Quant Electron* 2014;46:1165–77.
- [14] Youplao P, Pornsuwancharoen N, Amiri I, Jalil M, Aziz M, Ali J, Singh G, Yupapin P, Grattan K. Microring stereo sensor model using Kerr-Vernier effect for bio-cell sensor and communication. *Nano Commun Networks* 2018.
- [15] Phatharacorn P, Chiangga S, Yupapin P. Analytical and simulation results of a triple micro whispering gallery mode probe system for a 3D blood flow rate sensor. *Appl Opt* 2016;55:9504–13.
- [16] Prabhu AM, Tsay A, Han Z, Van V. Extreme miniaturization of silicon add-drop microring filters for VLSI photonics applications. *IEEE Photon J* 2010;2:436–44.
- [17] Liu K, Sun S, Majumdar A, Sorger VJ. Fundamental scaling laws in nanophotonics. *Sci Rep* 2016;6:37419.
- [18] Pornsuwancharoen N, Youplao P, Aziz M, Ali J, Amiri I, Punthawanunt S, Yupapin P, Grattan K. In-situ 3D micro-sensor model using embedded plasmonic island for biosensors. *Microsyst Technol* 2018:1–5.
- [19] Pornsuwancharoen N, Amiri I, Suhailin F, Aziz M, Ali J, Singh G, Yupapin P. Micro-current source generated by a WGM of light within a stacked silicon-graphene-Au waveguide. *IEEE Photon Technol Lett* 2017;29:1768–71.
- [20] Atabaki AH, Moazeni S, Pavanello F, Gevorgyan H, Notaros J, Alloatti L, Wade MT, Sun C, Kruger SA, Meng H. Integrating photonics with silicon nanoelectronics for the next generation of systems on a chip. *Nature* 2018;556:349.
- [21] Koos C, Jacome L, Poulton C, Leuthold J, Freude W. Nonlinear silicon-on-insulator waveguides for all-optical signal processing. *Opt Express* 2007;15:5976–90.
- [22] Smektala F, Quemard C, Leneindre L, Lucas J, Barthélemy A, De Angelis C. Chalcogenide glasses with large non-linear refractive indices. *J Non-Cryst Solids* 1998;239:139–42.
- [23] Poznanski R, Cacha L, Al-Wesabi Y, Ali J, Bahadoran M, Yupapin P, Yunus J. Solitonic conduction of electrotonic signals in neuronal branchlets with polarized microstructure. *Sci Rep* 2017;7:2746.
- [24] Ali J, Youplao P, Pornsuwancharoen N, Jalil M, Chaiwong K, Aziz M, Amiri I, Bunrungses M, Singh G, Yupapin P. On-chip electro-optic multiplexing circuit using serial microring boxcar filters. *Results Phys* 2018;10:18–21.